

## Photoemission Studies of the Noble Metals. II. Gold\*†

W. F. KROLIKOWSKI

*Stanford University, Stanford, California 94305*

and

*Cogar Corp., 22 Oakley, Poughkeepsie, New York 12600‡*

AND

W. E. SPICER

*Stanford University, Stanford, California 94305*

(Received 22 July 1969)

New photoemission data have been obtained from evaporated films of gold in the range of photon energies between 5 and 21.2 eV. With the exception of a single direct transition, all the optical transitions appear to fit a nondirect model; consequently, it has been possible to construct an optical density of states (ODS) for gold in the region  $\pm 11.6$  eV about the Fermi level  $E_F$ . Two broad peaks dominate the valence ODS. These are centered at about 3.5 and 6 eV below  $E_F$ . The higher-lying peak is resolved into a doublet with peaks at 3.0 and 3.8 eV. The two broad peaks correlate well with peaks observed in soft-x-ray photoemission. Positive correlation is also found with band calculations. The electron-electron scattering length for gold has been calculated as a byproduct of the analysis relating the ODS to the photoemission data, and detailed quantitative agreement is found between the calculated scattering length and Kanter's experimental values in the range between 5 and 11 eV above the Fermi level. This quantitative agreement between the calculated and experimental scattering length provides a useful cross-check in support of both the experimental data and the model used to analyze them.

## I. INTRODUCTION

EXPERIMENTAL measurements have been made of the quantum yield and photoelectric energy distribution curves (EDC's) from gold in the range of photon energies between 5 and 21.2 eV, and from this data an optical density of states (ODS) in the region  $\pm 11.6$  eV about the Fermi level has been constructed. The analysis of the gold data is based upon the details of the nondirect transition method of analysis described earlier by Krolkowski and Spicer.<sup>1</sup> A comprehensive discussion of the general approach as well as the mathematical details of the calculations presented in this paper for gold can be found in Ref. 1. There are several ways the gold work differs from the copper study presented in Ref. 1 and earlier by Berglund and Spicer.<sup>2,3</sup> Since gold reacts with cesium,<sup>4</sup> it was not possible to reduce the gold work function by a cesium surface layer. As a result, it was not possible to examine by photoemission the conduction band in the energy range  $1.5 \lesssim E - E_F \lesssim 5.5$  eV ( $E_F$  is the Fermi energy) as was the case for Cu with Cs on the surface. Useful EDC's were only obtained for  $h\nu \geq 7.4$  eV. This was due

to the low yield near the threshold for photoemission and to the necessity of obtaining electrons at high enough energy so that their escape probability is not a fast function of their energy as is the case near the threshold for emission.<sup>1</sup> For final-state energies 7.4 eV or more above the Fermi surface, the leading edge of the distribution is found to be much less well defined than at lower energies. Principal causes of this are probably the short electron-electron scattering length at these energies and the decrease in instrumental resolution with increased electron kinetic energy.<sup>5</sup> As a result, it is much more difficult to obtain an accurate estimate of the ODS in Au than in Cu.

Although measurements for Au could not be carried as far into the visible as for Cu, they were extended farther (to 21.3 eV) into the ultraviolet by means of a new type of tube described in the next section. This was important because of the long valence bandwidth of Au.

One product of our analysis of the photoemission and optical data is the electron-electron scattering length  $L(E)$  as a function of energy. There were no experimental data for Cu to which our results could be compared; however, in the case of Au such data are available<sup>6-8</sup> and give an additional check on the data and analysis. Detailed agreement is obtained.

Our presentation of material in this paper will be similar to that used in Ref. 1. After a brief outline of the experimental and analytical methods, the derived ODS will be presented and a large number of curves given

\* Work supported in part by National Aeronautics and Space Administration, Advanced Research Projects Agency through the Center for Materials Research at Stanford University, National Science Foundation, and the Cogar Corp.

† Based largely on a thesis submitted by W. F. Krolkowski to Stanford University in partial fulfillment of the requirements for a Ph.D. degree.

‡ Present address.

<sup>1</sup> W. F. Krolkowski and W. E. Spicer, Phys. Rev. (to be published).

<sup>2</sup> C. N. Berglund and W. E. Spicer, Phys. Rev. **136**, A1030 (1964).

<sup>3</sup> C. N. Berglund and W. E. Spicer, Phys. Rev. **136**, A1044 (1964).

<sup>4</sup> W. E. Spicer, A. H. Sommer, and J. G. White, Phys. Rev. **115**, 57 (1959).

<sup>5</sup> T. DiStefano and D. Pierce (private communication).

<sup>6</sup> H. Kanter, Phys. Rev. B **1**, 522 (1970).

<sup>7</sup> C. R. Crowell and S. M. Sze, in *Physics of Thin Films*, edited by G. Hass and R. E. Thun (Academic Press Inc., New York, 1967), Vol. 4.

<sup>8</sup> S. M. Sze, J. L. Moll, and T. Sugano, Solid State Electron. **7**, 509 (1964).

comparing the results of calculations based on the ODS with experimental results. Finally, a comparison will be made with other estimates of the density of states.

## II. EXPERIMENTAL TECHNIQUES

In the range of photon energies between 5 and 11.6 eV, the experimental apparatus and techniques were essentially the same as those described in Ref. 1, except that the films were prepared and tested at pressures of about  $5 \times 10^{-9}$  Torr. At photon energies higher than 11.6 eV, EDC's were measured by means of a "knock-off tube,"<sup>9</sup> which is a specially constructed photodiode with a LiF window that is connected to the tube body with a very thin glass neck. The knock-off tube was used in the following manner. First, the tube was evacuated to a pressure of, typically,  $5 \times 10^{-9}$  Torr, the gold film evaporated, and the tube sealed off. To avoid contamination, this processing was done using an ion-pump vacuum system. The tube was then placed in an evacuated chamber that was attached to the vacuum monochromator; this monochromator-chamber system was differentially pumped with a liquid nitrogen baffled oil-diffusion pump so that during operation the pressure in the chamber surrounding the tube was only  $2 \times 10^{-5}$  Torr, whereas the pressure in the monochromator was  $1 \times 10^{-4}$  Torr. The monochromator pressure of  $1 \times 10^{-4}$  Torr was due almost entirely to the gas (typically hydrogen, helium, or argon) from the Hintegger lamp; with the gas not flowing through the lamp, the pressure in the monochromator was less than  $1 \times 10^{-7}$  Torr. In the actual experiment, photoemission data were first taken at photon energies up to 11.6 eV, while the LiF window on the knock-off tube was still intact and the gold film still under ultrahigh vacuum. The LiF window was then knocked off the tube using a guillotineline apparatus, exposing the gold film directly to the light beam and a vacuum of  $2 \times 10^{-5}$  Torr. Energy distribution curves at photon energies up to 21.2 eV were quickly made before the gold could become too seriously contaminated. A more complete description of the knock-off tube experiment can be found in Ref. 9.

## III. ANALYSIS OF PHOTOEMISSION DATA

The photoemission data for gold has been analyzed in terms of nondirect transitions and an ODS having a free-electron-like conduction band and a semiclassical threshold function, in the manner of the analysis for copper.<sup>1</sup> As shown in Ref. 1, the EDC's  $\eta(E, h\nu)$ , the quantum yield  $Y(h\nu)$ , the electron-electron scattering length  $L(E)$ , and the optical constant  $\epsilon_{2b}(h\nu)$  can be related to the ODS by the following relationships:

$$\eta(E, h\nu) = C[\alpha(h\nu)L(E), T_f(E)]T_f(E) \times \left( \frac{\alpha(h\nu)L(E)}{\alpha(h\nu)L(E)+1} \right) N_c(E)N_v(E-h\nu) / \int_{E_F}^{E+h\nu} N_c(E)N_v(E-h\nu)dE, \quad (1)$$

$$Y(h\nu) = \int_{\varphi}^{h\nu} \eta(E, h\nu)dE, \quad (2)$$

$$L(E) = K|v_g(E)| / \int_{E_F}^{2E_F-E} d(E\nu^0) \int_{E_F-E\nu^0}^{(1/2)(E-E\nu^0)} N_v(E\nu^0) \times N_c(E-\Delta E)N_v(E\nu^0+\Delta E)d(\Delta E), \quad (3)$$

and

$$\epsilon_{2b}(h\nu) = \frac{A}{\nu^2} \int_{E_F}^{E_F+h\nu} N_c(E)N_v(E-h\nu)dE, \quad (4)$$

where  $\alpha(h\nu)$  is the absorption coefficient;  $N_c(E)$  is the conduction band part of ODS;  $N_v(E)$  is the valence band part of ODS;  $\varphi$  is the work function;  $E_F$  is the Fermi energy;  $K$  is the arbitrary normalizing constant;  $A$  is the arbitrary normalizing constant (including square of matrix element);  $v_g = 2(E-E_B)/m$  is the free-electron group velocity;  $E_B$  is the location of bottom of free-electron-like conduction band; and  $T_f(E) = \frac{1}{2}[1 - (\varphi - E_B/E)^{1/2}]$  is the semiclassical threshold function appropriate to free-electron-like conduction band. The factor  $C$  can vary only between 0.5 and 1.0, and is given by

$$C[\alpha(h\nu)L(E), T_f(E)] = \frac{\alpha L + 1}{\alpha L} - \frac{\alpha L + 1}{2(T_f)(\alpha L)^2} \times \ln \left( \frac{\alpha L + 1}{\alpha L + 1 - 2\alpha L T_f} \right). \quad (5)$$

In our calculations, we have used the data of Ref. 10 for  $\alpha(h\nu)$ , and have used the data of Refs. 10-12 for the reflectivity  $R(h\nu)$ , which was used to correct the experimental yield for reflection.

## IV. OPTICAL DENSITY OF STATES OF GOLD

The valence ODS for gold obtained in this work is given in Fig. 1, where the ODS for the conduction

<sup>10</sup> L. R. Canfield, G. Hass, and W. R. Hunter, J. Phys. (Paris) **25**, 124 (1964).

<sup>11</sup> B. R. Cooper, H. Ehrenreich, and H. R. Philipp, Phys. Rev. **138**, A494 (1965).

<sup>12</sup> *American Institute of Physics Handbook*, edited by D. E. Gray (McGraw-Hill Book Co., New York, 1963), 2nd ed. Chap. 6, p. 119.

<sup>9</sup> W. F. Krolkowski, Ph.D. thesis, Stanford University, 1967 (unpublished). May be obtained by writing University Microfilms Library Services, 300 N. Zeeb Road, Ann Arbor, Mich. 48106 and asking for call number 65-11813.

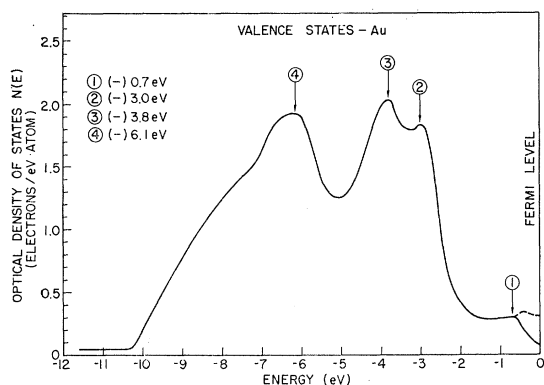


FIG. 1. Optical density of states (ODS) for the gold valence band. There is considerable uncertainty in the curve for energy less than  $-7$  eV.

states is given in Fig. 2. The absolute scale on the valence ODS was obtained by normalizing the area under the curve to the 11 valence electrons of Au.

As mentioned in the Sec. I, the leading edge of the Au EDC's is probably smeared out artificially. The solid curve in Fig. 1 was obtained directly from the EDC's with no attempt to take this into account. As a result there is a dip in the ODS near  $E_F$  which does not appear to be physically reasonable. For example, the value for density of states at  $E_F$  is 0.06 electrons/eV atom as opposed to the specific-heat value of 0.32 electrons/eV atom.<sup>13</sup> Although there are physical arguments (phonon-electron interactions, etc.) why the latter should be higher than the former, a factor-of-5 difference is clearly much too high. In Cu,<sup>1</sup> where measurements could be made for  $h\nu \geq 1.6$  eV, no such discrepancy was found. In the insert to Fig. 1 we have sketched in a reasonable adjustment of the ODS which preserves the structure near 0.5 eV and makes the ODS at  $E_F$  equal to the value obtained from specific heat.

As in all cases of ultraviolet photoemission studies, ODS cannot be obtained with high precision for states more than 5 eV below the Fermi level. However, in this case ample evidence is found for the broad peak at 6.1 eV below the Fermi level. In other cases<sup>1,14,15</sup> it has been argued that such peaks are due to plasmon excitation or other non-one-electron events; however, as will be shown in Sec. IX the occurrence of a peak near 6 eV is quite compatible with band calculations and a similar peak has been seen in soft-x-ray photoemission. Thus, it seems likely that the broad peak 6.1 eV below the Fermi level is due to a peak in the density of states.

Let us now examine the conduction band ODS (Fig. 2). As mentioned in Sec. I, no direct information could be obtained on the conduction band for  $0 \leq E - E_F \leq 5.0$  eV. Between 0 and 2 eV, the ODS was obtained by

extrapolating the curve from the valence states. Since the valence ODS is not well determined near  $E_F$  this is a questionable process. In the subsequent sections a number of quantities will be presented which have been calculated on the basis of the ODS and nondirect model. Of these only  $\epsilon_2$  in the range  $2.5 \lesssim h\nu \leq 3.5$  eV will depend strongly on this conduction ODS near  $E_F$ ; however, the agreement between experiment and calculation would not be so good if the ODS did not drop sharply between 0 and 1 eV. However, better agreement could have been obtained between calculation and experiment if a peak was placed in the ODS 2 eV above the Fermi level. This is indicated in Fig. 2; however, no such peak was used in the calculation.

Above 2 eV, a free-electron-like density of states<sup>1</sup> was used as a first approximation. This is indicated by a solid line where no other structure was superimposed on it and by a dashed line where such structure is superimposed. The energy dependence of the ODS, which results from this free-electron approximation, was sufficiently slow so that it had no significant effect on the calculations done. Placing the bottom of the free-electron band at the Fermi level rather than at the bottom of the valence band did have some effect on the escape function  $T_f$  (see Sec. III). However, it was found that significantly better agreement with experiment was obtained if it was placed at the Fermi level rather than at the bottom of the valence band; therefore, this procedure was used here.

Whereas an absolute scale could be put on the valence ODS by equating its area to 11 electrons/atoms, there is no satisfactory procedure for putting such a scale on the conduction band ODS of Au. Fortunately, such a scale is not necessitated by any of the calculations performed here (see Sec. III); therefore, Fig. 2 just presents the relative density of states.

## V. ELECTRON-ELECTRON SCATTERING LENGTH IN GOLD

A plot of  $L(E)$ , the mean free path of electron-electron scattering, is presented in Fig. 3. The relative values of  $L(E)$  were obtained from Eq. (3) (Sec. III) and the ODS of Figs. 1 and 2<sup>1</sup> and Ref. 9 for further details. An absolute value was placed on the curve by using Eq. (2) and the experimentally determined value

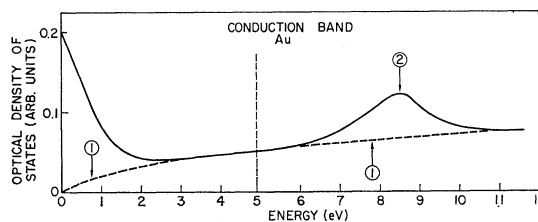


FIG. 2. The ODS of gold for the conduction states within 11.5 eV of the Fermi energy. The zero of energy is taken at the Fermi level. The dashed curve labeled ① is a free-electron density of states with its minimum at the Fermi level.

<sup>13</sup> C. Kittel, in *Introduction to Solid-State Physics* (John Wiley & Sons, Inc., 1956), p. 259.

<sup>14</sup> R. K. Nesbet and P. M. Grant, *Phys. Rev. Letters* **19**, 222 (1967).

<sup>15</sup> T. A. Callcott and A. U. McRae, *Phys. Rev.* **178**, 966 (1969).

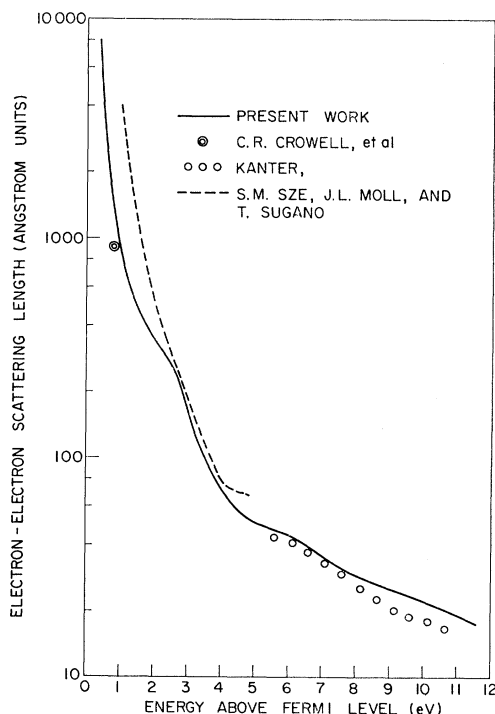


FIG. 3. Values of the electron-electron scattering length  $L(E)$ . The absolute results obtained in this work compare favorably with those obtained by Crowell and Sze (Ref. 7), Kanter (Ref. 6), and Sze, Moll, and Sugano (Ref. 8).

of yield at 8.6 eV. Having obtained the ODS as described in the last section,  $L(E)$  was the only quantity on the right-hand side of Eq. (2) which was not determined.

For Cu there was no other reliable determination of  $L(E)$  to which the values determined in our studies could be compared. Fortunately, this is not the case for Au. We present in Fig. 3 the results obtained from the publications of Kanter<sup>6</sup>; Crowell and Sze<sup>7</sup>; and Sze, Moll, and Sugano.<sup>8</sup> The agreement between our calculated curve and the experimental data is seen to be remarkably good over a wide range of energies. For the purposes of photoemission studies on clean gold, the most important region of energies is between 5.0 and 11.6 eV above the Fermi level, and in this region there is excellent agreement between the calculated  $L(E)$  and the data points of Kanter.<sup>6</sup> Kanter studied the transmission measurements of electron beams through thin gold films and his results are thought to be quite reliable. Not only is the magnitude of our  $L(E)$  very close to Kanter's measurements, but there also appears to be detailed agreement with regard to structure in the curves. In both the calculated curve and the experimental data there is a significant drop in  $L(E)$  at an energy of about 6.5 eV above the Fermi level. As seen from the ODS of Fig. 1, this decrease in  $L(E)$  is due to the onset of scattering between the photoexcited electrons and the large number of valence electrons constituting peak ④ in Fig. 1.

The good agreement is very encouraging since our values depend on the ODS determined in this work. Although they also depend on the assumption of nondirect transitions in the electron scattering process, this assumption may not be too important. Kane<sup>16</sup> obtained values of  $L(E)$  for Si which were independent of the requirement of conservation in the scattering process.

If structure in the curve is disregarded, the calculated  $L(E)$  of Fig. 3 is found to be quite well approximated by an  $E^{-3/2}$  dependence. In fact, it can readily be shown<sup>9</sup> from Eq. (3) that at energies well above the Fermi level any material (metal, insulator, or semiconductor) with an arbitrary valence band ODS and a free-electron-like conduction band envelope (proportional to  $E^{1/2}$ ) may be expected to have an  $L(E)$  with approximately an  $E^{-3/2}$  energy dependence.

The remarkable agreement between the calculated  $L(E)$  and the experimental data points for gold strongly support the validity of the method described in Ref. 1, which we have used to analyze photoemission data from a number of different materials<sup>1,9</sup> for which there are no reliable experimental values of  $L(E)$ .

## VI. PHOTOEMISSION FROM GOLD

The experimental and calculated quantum yields are compared in Fig. 4, where it is seen that the agreement with respect to both shape and magnitude is excellent.

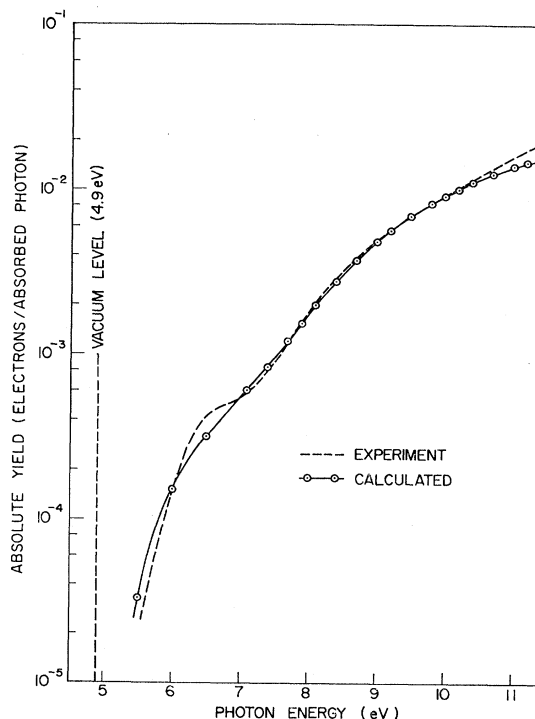


FIG. 4. Calculated and experimental yield from gold.

<sup>16</sup> E. O. Kane, Phys. Rev. **159**, 624 (1967).

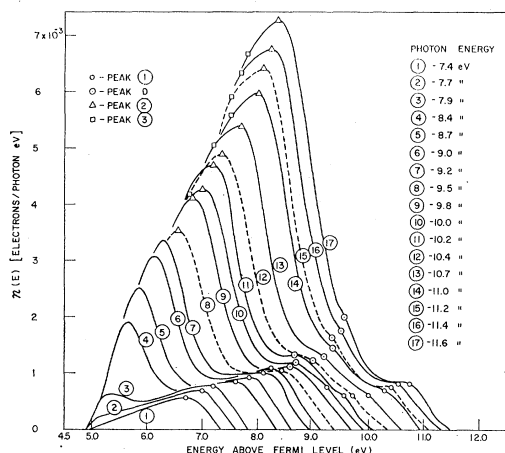


FIG. 5. A family of energy distribution curves (EDC's) for gold in the range  $7.4 \leq h\nu \leq 11.6$  eV. The EDC's have been normalized to yield. Peaks ①, ②, and ③ correspond to peaks in the valence ODS of Fig. 1. Peak D is due to a direct transition believed to originate near the  $L_2'$  symmetry point. These data were taken under good vacuum conditions.

The calculated quantum yield has been obtained from Eq. (2) using the ODS of Fig. 1 and the calculated electron-electron scattering length of Fig. 3. One of the most significant features of the quantum yield for gold is that it is relatively small, being only about 2% at a photon energy of 11.6 eV above the Fermi level. This small value of the photoelectric yield is due mainly to the small value of the free-electron threshold function  $T_f(E)$  and the short electron-electron scattering length  $L(E)$ . Because  $T_f(E)$  and  $L(E)$  are quite similar for both gold and copper, the gold yield of Fig. 4 is seen to be quite similar to the copper yield presented in Ref. 1.

The only significant structure in the yield curve for gold is a fairly pronounced rise which begins at a photon energy of about 7.5 eV. This rise is evident in both the calculated and the experimental curves, and is due to the onset of photoemission from  $d$ -band peak ② of Fig. 1.

We will next consider the EDC's. Of central importance here is the comparison between the experimental EDC's and those calculated from the ODS on the basis of nondirect transitions. However, before presenting these results, we will attempt to give an over-all view of the EDC's with particular emphasis on identifying direct transitions since these are not taken into account in the calculated EDC's. In addition, we will attempt to show the general features of the non-direct portion of the EDC's in order to make clear the general features of the ODS.

The results of energy distribution measurements are shown in Figs. 5–11. In Fig. 5 the EDC's obtained from clean Au for various values of photon energy are plotted versus the energy of the electrons with respect to the Fermi level. In order to give the reader a good overview of the manner in which structure in the EDC's moves

with photon energy, a plot is presented in Fig. 6 of the kinetic energy of the peaks as a function of photon energy. In Figs. 7 and 8, EDC's taken in poorer vacuum for  $h\nu = 16.8$  and 21.2 eV are presented. Figures 9 and 10 give EDC's taken under different conditions and from different samples. In Fig. 11 we compare the measured EDC's with those calculated using the ODS of Figs. 1 and 2 and the nondirect model outlined in Sec. III.

Figure 5 shows a family of experimental EDC's for  $7.4 \leq h\nu \leq 11.6$  eV. Note that the scale on the ordinate is absolute. The conduction band ODS (Fig. 2) contains a broad peak centered at 8.5 eV. Let us next examine the evidence in Fig. 5 for this peak. Due to the combined effect of escape probability  $T(E)$  (see Sec. III) and the electron-electron scattering length (see Fig. 3), the height of the EDC's usually increase for about the first 2 eV above threshold; then the height becomes relatively constant. This was, for example, the situation in copper<sup>1</sup> where the height of the first  $d$  peak (peak ② in Fig. 5) increased by a factor of 4 for  $8.6 < h\nu < 8.8$  and then became almost constant for  $8.8 \lesssim h\nu \lesssim 11.6$  eV. If one follows the first  $d$  peak in Au, a very different situation is seen. While some tendency to level off occurs between final-state energies  $E$  of 7 and 8 eV, the peak increases rather sharply for  $8 < E < 9$  eV. The behavior of the peak due to the  $s$ - and  $p$ -derived states (peak ① in Fig. 5) is somewhat more complicated due to the appearance of direct transition near  $E = 9.0$  eV. However, if the effects of the direct transitions are ignored, we see a similarity in the behavior of peak ① and ② between 8 and 9 eV. More striking, though, is the decrease in peak ① for final states near 9.5 eV.

The peaking of the EDC's near 8.5 eV described in the last paragraph<sup>7</sup> has led us to postulate the broad peak in the final ODS centered at about  $E = 8.5$  eV in Fig. 2

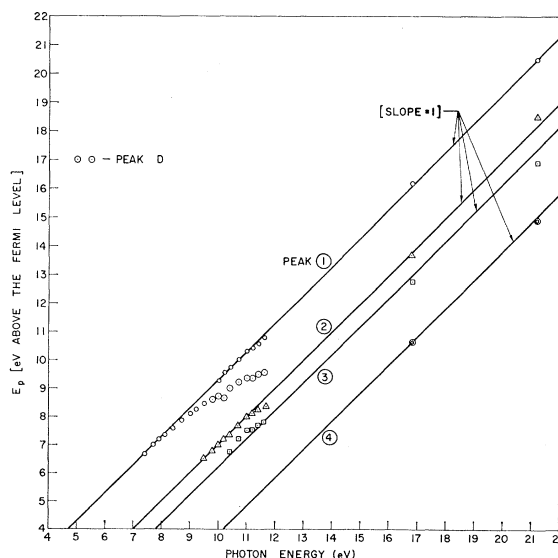


FIG. 6. Plots of the final energy of the peaks in Fig. 5 versus the photon energy.

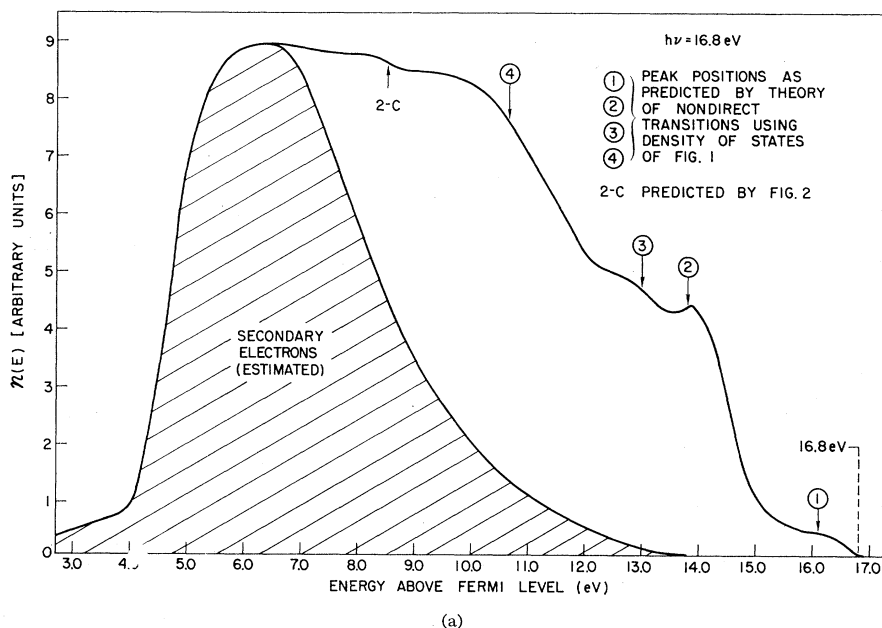
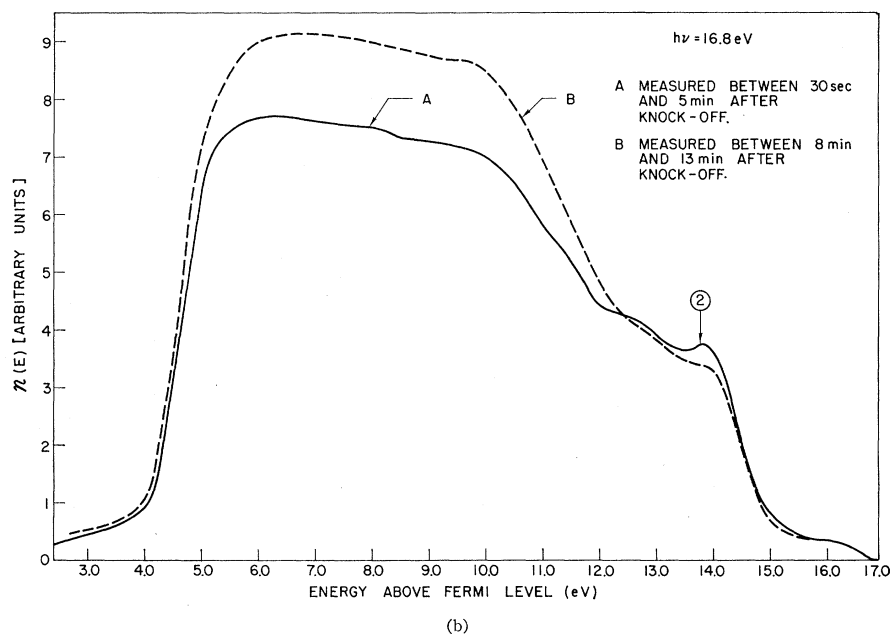


FIG. 7. (a) Experimental energy distribution curve for gold obtained using a knock-off tube. The measurement of this curve was begun 30 sec after knock off, and completed within 5 min after knock off; (b) energy distribution curves showing deterioration with time shortly after LiF window had been knocked off.



(peak ②). Including this peak in the ODS improved the agreement between the calculated and measured EDC's. As will be seen later, correlation is found between this peak and a flat band in the calculated density of states.

The peaks in the experimental EDC's of Fig. 5 are labeled according to the notation of the ODS of Fig. 1. In Fig. 6 the final-state energy of these peaks is plotted as a function of photon energy in the range of photon energies between 7.4 and 21.2 eV. The points at 16.8 and 21.2 eV were obtained from the low vacuum knock-off tube experiments, Figs. 7 and 8.

As seen from Figs. 5 and 6, the valence band peak ① splits into two peaks for  $h\nu \gtrsim 8.8$  eV. One of the peaks

(peak ①) moves in the manner of nondirect transitions, where  $\Delta E_p = \Delta h\nu$ . The other peak, called peak D, has the nature of a direct transition, where  $\Delta E_p \neq \Delta h\nu$ . At the onset of this direct transition, the initial states are about 0.8 eV below the Fermi level,  $E_F$ , and the final states about 8 eV above  $E_F$ . Similar transitions have been observed in Cu and definitively associated with the region of the zone near the L point. In Fig. 2 it can be seen that  $L_2'$  point is located about 0.7 eV in good agreement with the observed initial state; however, Marshall's band calculations locate the final state,  $L_1$ , about 6.0 eV above  $L_2'$  and not about 8.8 eV as obtained from our measurements. The experimental results sug-

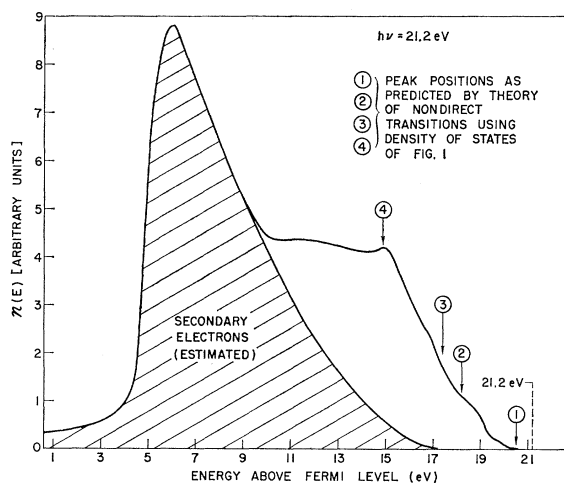


FIG. 8. Experimental energy distribution curve for gold obtained using a knock-off tube. The measurement was made 3 h after the LiF window was knocked off.

gest that  $L_1$  is located about 8 eV above the Fermi surface; however, the possibilities that the direct transition occurs somewhere in the zone or that it is to a  $L$  conduction lying above  $L_1$  cannot be completely ruled out at this time.

From Figs. 5 and 6 it can be seen that the valence band peaks ①, ②, ③, and ④ move in the manner of nondirect transitions in the range of photon energies between 7.4 and 11.6, and above 16.8 eV, indicating that in these regions the data are consistent with the nondirect model, with the exception of a single direct transition from  $s$ - and  $p$ -derived initial states mentioned above.

In Figs. 7 and 8 we present data at 16.8 and 21.2 eV obtained from the knock-off tube described in Sec. II. This allowed us to use larger values of  $h\nu$  than the LiF would transmit and thus to probe deeper into the valence states. For example, peak ④ in the valence band ODS could not be clearly identified in the photoemission

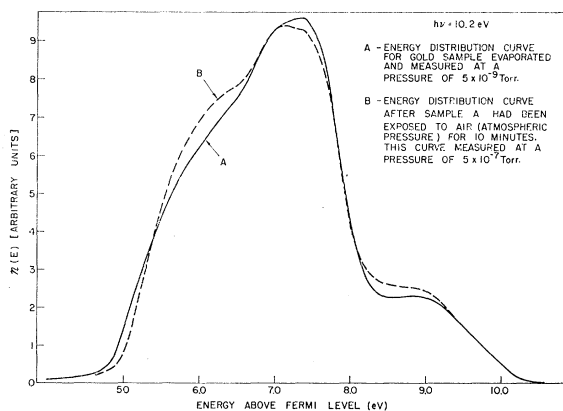


FIG. 9. Energy distribution curves before and after gold sample was exposed to air. Exposure to air caused the photoelectric yield to change by less than 1% at this photon energy.

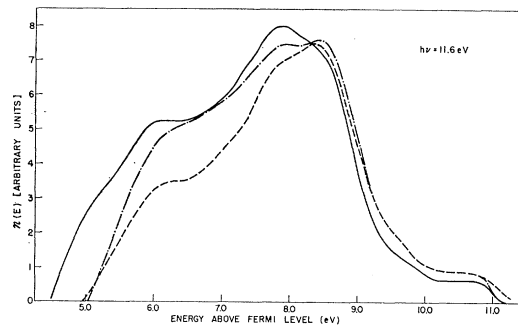


FIG. 10. Comparison of shapes of energy distribution curves for three different samples of gold.

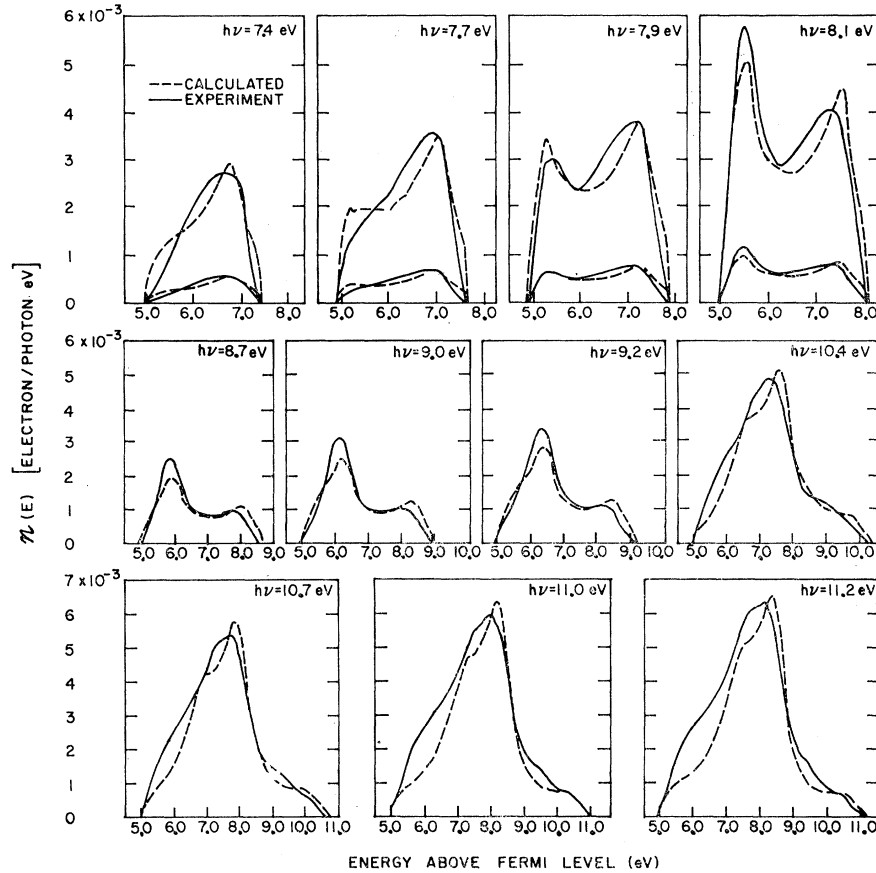
experiments from clean gold, because of the limitations of the LiF window, but could be clearly seen in the low vacuum knock-off tube experiments, as seen in Figs. 7 and 8. Peak ③, which is seen in Fig. 5 only as a shoulder, shows up more distinctly in Figs. 7 and 8. Note also in Fig. 7 that the conduction band peak at 8.5 eV (peak ② in Fig. 2) is identified as distinct structure, whereas in Fig. 5 this peak could be identified only by the amplitude modulation of valence band structure. Even though gold is quite insensitive to contamination, the vacuum conditions in our windowless experiments were apparently sufficiently adverse to cause rapid deterioration of the EDC's, as shown in Fig. 7; fortunately, a limited number of good measurements could be made before the contaminating effects obliterated the structure in the EDC's.

Although some contamination resulted in the gold films studied in the oil-pumped knock-off tube experiments (see Sec. II), the EDC's for gold appear to be quite insensitive to air. Figure 9 compares two EDC's at a photon energy of 11.6 eV: EDC A was measured from a freshly prepared film at ultrahigh vacuum, and EDC B was measured from the same gold film after it had been exposed to air at atmospheric pressure. Both measurements were made in an oil-free vacuum system, and from the close agreement between the two curves, it must be concluded that EDC's from gold are very insensitive to exposure to air.

Figure 10 compares EDC's from several different samples of gold. The EDC's are quite similar in their main features. Note that in one case, the work function was only about 4.5 eV, and that photoemission from the deep-lying valence band peak ④ is more evident than in the other two curves.

In Fig. 11 the calculated EDC's are compared with the experimental EDC's for gold in the range of photon energies between 7.4 and 11.6 eV. The calculated curves were obtained from Eq. (1) using the ODS of Figs. 1 and 2 and the calculated electron-electron scattering length of Fig. 3. The curves of Fig. 11 show that the over-all agreement between the calculated and the experimental EDC's is very good with regard to both shape and magnitude. However, the detailed agreement

FIG. 11. Comparison of calculated and measured EDC's for  $7.4 \leq h\nu \leq 11.2$  eV. For  $7.4 \leq h\nu \leq 8.1$  eV, an enlarged set of curves is given by multiplying the absolute curves times 5. For additional curves see Ref. 9.



between theory and experiment is not quite as good as that obtained for copper. As expected, the nondirect model does not explain the peak location for the direct transitions to final states in the conduction band between 8 and 9 eV above the Fermi level. Nevertheless, the nondirect model and the ODS of Figs. 1 and 2 appear to account very well for the over-all characteristics of the experimental EDC's in the range of photon energies between 7.4 and 11.6 eV.

## VII. OPTICAL CONSTANT $\epsilon_{2b}$

The shape of  $\epsilon_{2b}$  that is obtained from Eq. (4) using the ODS of Figs. 1 and 2 is compared, in Figs. 12(a)–12(c), to experimental curves. The major features of the calculated curve are the rather flat-topped peak in the region between 3 and 4 eV and a strong shoulder at 6.5 eV. The flat peak between 3 and 4 eV is due to strong transitions from valence band peaks ② and ③ to empty states just above the Fermi level, and the shoulder at 6.5 eV is due to strong transitions from valence band peak ④ to the same final states.

Since the published experimental values of  $\epsilon_{2b}$  vary somewhat from author to author, we have found it necessary to compare our calculated  $\epsilon_{2b}$  with the ex-

perimental data<sup>11,17,18</sup> of several authors, as shown in Figs. 12(a)–12(c). Figure 12(a) shows that the corners of the calculated peak at about 3 and 4 eV are in rather good agreement with the two experimentally observed peaks at 3.1 and 3.8 eV. However, the experimentally observed shoulder at 2.2 eV in Fig. 12(b) does not appear in the calculated  $\epsilon_{2b}$ . In Fig. 12(b) the agreement between theory and experiment is good between 2.5 and 6 eV, but there is a glaring discrepancy in that a large peak occurs in the experimental data at a photon energy of 8.0 eV, and no such peak appears in the calculated  $\epsilon_{2b}$ ; this discrepancy is also evident in Fig. 12(c).

Thus, we see that the ODS of Fig. 1 is able to account for the broad peak in  $\epsilon_{2b}$  between 3 and 4 eV, but is not able to account for the very strong peak at 8.0 eV. This discrepancy may be due to the present lack of information about structure that may exist in the unexplored region between the Fermi level and 4.9 eV above the Fermi level or to other factors such as the assumption of constant matrix elements. Because of the similarities in the EDC's from copper<sup>1</sup> and gold, it is possible that there exists a peak in the conduction band ODS for gold

<sup>17</sup> M. Garfinkel, J. J. Tiemann, and W. E. Engeler, Phys. Rev. **148**, 695 (1966).

<sup>18</sup> D. Beaglehole, Proc. Phys. Soc. (London) **85**, 1007 (1965).



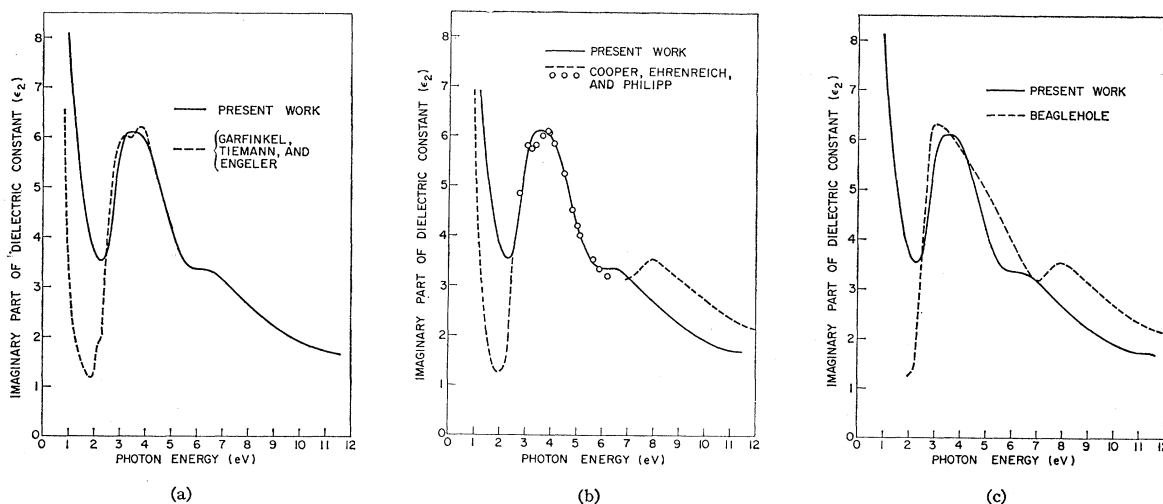


FIG. 12. (a) Comparison of calculated  $\epsilon_2$  with the  $\epsilon_2$  of Garfinkel, Tiemann, and Engeler (Ref. 17); (b) Comparison of calculated  $\epsilon_2$  with the  $\epsilon_2$  of Cooper, Ehrenreich, and Philipp (Ref. 11); (c) Comparison of calculated  $\epsilon_2$  with Beaglehole's  $\epsilon_2$  (Ref. 18).

at an energy of about 2 eV above the Fermi level, just as in the case of copper. If such a peak does exist, then the  $\epsilon_{2b}$  calculated from the ODS would account qualitatively for all the major features in the experimental data, including the peaks at 2.2 and 8.0 eV. However, the existence of peak *P* must remain a conjecture until either proved or disproved by future experiments in the unexplored region of the conduction band. The discrepancy between the calculated and measured  $\epsilon_2$  near 8 eV might also be due to an inadequacy of the nondirect model such as the assumption of constant matrix elements.

## VIII. COMPARISON OF ODS TO RESULTS OF OTHER WORK

### Comparison of ODS to Results of Band Calculations

We have found it possible to make some correlation between structure in the gold ODS and flat bands in the calculated band structure of Marshall *et al.*,<sup>19</sup> as shown in Fig. 13. In Fig. 13 the shaded bars represent the location of structure in the ODS of Figs. 1 and 2 and it is seen that these shaded bars correspond fairly closely to features in the calculated band structure. Consequently, we have associated the strong valence band peaks ②, ③, and ④ with states derived largely from the 5*d* atomic wave functions. These identifications with band structure are qualitatively similar to identifications made earlier for copper.<sup>1</sup>

### Comparison with Soft-X-Ray Photoemission Work

In Fig. 14 we compare the valence ODS of states with results obtained by Siegbahn *et al.*<sup>20</sup> from soft-x-ray photoemission work. As can be seen, relatively good agreement is obtained between the two results. The two major peaks are relatively similar. There is a difference in the relative strength of these two peaks; however, this is probably not significant since constant matrix elements must be assumed to hold if the peak heights are to be compared and the relative strength of peak ④ in Fig. 2 is difficult to determine. In the ODS the first peak is resolved into a doublet; whereas, this is just hinted at in the x-ray results. This difference may be

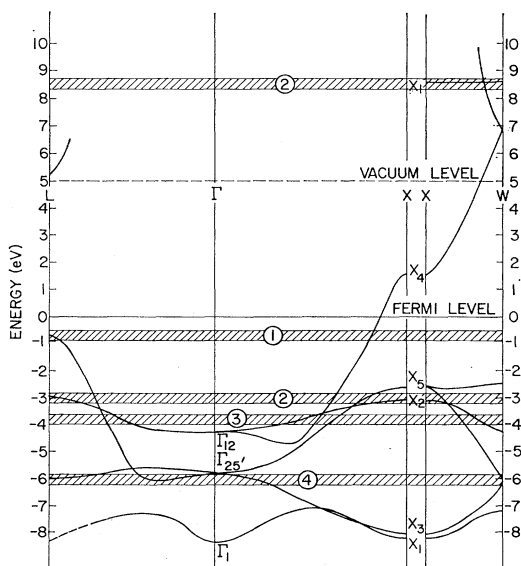


FIG. 13. The band structure of gold as calculated by Ballinger and Marshall (Ref. 19). The horizontal cross-hatched bars indicate the position of the peaks in the ODS found in the present work. The number assigned to these bars corresponds to the peaks in Figs. 1 and 2.

<sup>19</sup> R. A. Ballinger and C. A. W. Marshall, J. Phys. C 2, 1822 (1969).

<sup>20</sup> Kai Siegbahn, C. Norling, A. Fahlman, R. Nordberg, K. Hamrin, J. Hedman, G. Johansson, T. Bergmark, S. Karlsson, I. Lindgren, and B. Lindberg, in *ESCA Atomic, Molecular and Solid State Structure Studied by Means of Electron Spectroscopy* (Almqvist & Wiksells Boktryckeri AB, Uppsala, 1967), Ser. IV, Vol. 20.

due to the increased resolution obtainable in the photoemission work.<sup>1</sup>

### IX. DISCUSSION OF OPTICAL DENSITY OF STATES

In Sec. IX, an encouraging correlation was found between peaks in the valence ODS and flat regions in the calculated bands for Au. If the flat bands extend over much of the zone as Fig. 14 indicates, these would lead to peaks in the density of states. Correlations have been obtained previously between peaks in the ODS and calculated density of states for Cu and Ag.

Recently, Smith and Spicer<sup>21</sup> have reported calculations of the EDC's for Cu on the basis of direct transitions using a 0.4-eV broadening. They have found in this work that the position in energy of peaks in the calculated EDC's agree with those observed experimentally; however, the peak intensity is modulated more strongly than is observed experimentally or predicted by the nondirect model. Since the peaks in the EDC's calculated on the basis of direct transitions also coincide with peaks in the calculated density of states, it appears that the ODS has utility in presenting the results of photoemission measurement from narrow-band materials even if the transitions are direct in nature.

### X. CONCLUSIONS

We have found that the bulk of the photoemission data for gold is well described in terms of nondirect transitions and an ODS. As would be expected, the  $d$  states provide the most prominent structure in the ODS. Three strong pieces of structure are observed in the ODS of the  $d$  states: A broad peak centered at about 6.1 eV below the Fermi level  $E_F$ , and a doublet with peaks at about 3 and 3.8 eV below  $E_F$ . The over-all  $d$  width is 6 to 8 eV which is considerably wider than that of about 3 eV observed for Ag or about 4 eV estimated for Cu. Good correlation is obtained between the general features of the  $d$  states observed here and in the results of soft-x-ray photoemission (ESCS) studies.<sup>20</sup> Correlation is also found between the present results and band calculations.<sup>19</sup> Therefore, it appears likely that the valence ODS is closely correlated with the actual density of states of Au.

<sup>21</sup> N. V. Smith and W. E. Spicer, Opt. Commun. **1**, 157 (1969).

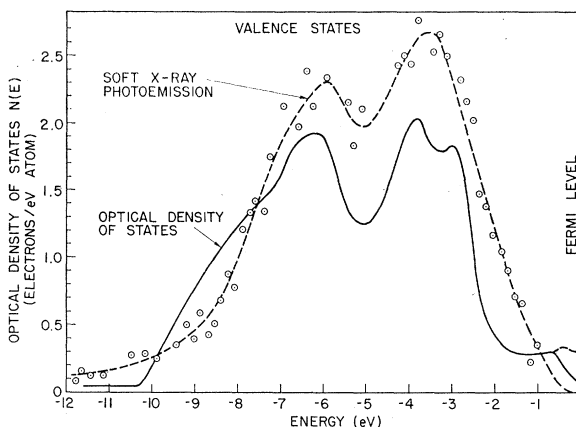


Fig. 14. Comparison of the ODS and the soft-x-ray photoemission results of Siegbahn *et al.* (Ref. 20). The x-ray results have been shifted to lower energy by 0.6 eV to obtain the best fit. (It is difficult to set the absolute zero of energy in the x-ray experiment.)

A single transition is observed, which is clearly direct. At the threshold for this transition, 8.8 eV, the initial states are located about 0.8 eV below  $E_F$  and the final states about 8 eV above  $E_F$ . It is suggested that this may be a  $L_{2'}$  to  $L_1$  transition similar to those reported previously in Cu<sup>1,3</sup> and Ag.<sup>3</sup>

The ODS for gold is found to account for some, but not all, of the major features in  $\epsilon_{2b}$ . This discrepancy may very well be due to structure in the as yet unexplored conduction band region between the Fermi level and 4.9 eV above the Fermi level.

The electron-electron scattering length  $L(E)$  obtained in this work for gold is found to be in remarkably good quantitative agreement with experimental results obtained by others<sup>6-8</sup> in the range of energies studied. This result is of importance, since it is an exacting check on the method described in Ref. 1 for analyzing photoemission data.<sup>1</sup> A value of 20 Å is obtained for  $L(E)$  for an electron 10 eV above  $E_F$ .

### ACKNOWLEDGMENTS

We would like to thank F. Peters and D. Mosher for developing the intricate glass techniques that made possible the construction of the knock-off tubes. We also wish to express our great appreciation to H. Kanter and C. A. W. Marshall, who made their results available before publication. Valuable conversations with Neville Smith are gratefully acknowledged.